Jurnal Matematika UNAND
Vol. **15** No. **3** Hal. 388 – 405
Edisi Juli 2026
ISSN : 2303–291X
e-ISSN : 2721–9410

https://doi.org/10.25077/jmua.15.3.388-405.2026

A MATHEMATICAL MODEL SEABRQ WITH OPTIMAL CONTROL FOR SOCIAL MEDIA ADDICTION INCORPORATING COGNITIVE DYSREGULATION

EVA SALSABILA, YUDI ARI ADI*

Program Studi Matematika, Universitas Ahmad Dahlan,
email : 2200015021@webmail.uad.ac.id, yudi.adi@math.uad.ac.id

Received April 23, 2026 Received in revised form July 18, 2026
Accepted July 19, 2026 Available online July 31, 2026

Abstract. This study proposes a SEABRQ compartmental model to analyze social media addiction transmission and its cognitive consequences, referred to as cognitive dysregulation or "brain rot." The total population is partitioned into six compartments: Susceptible (S), Engaged (E), Addicted (A), Cognitively Dysregulated (B), Regulated (R), and Quit (Q). R_0 is computed using the next generation matrix approach, and local asymptotic stability of both equilibrium points is established analytically. Sensitivity analysis identifies transmission rate and contact rate as the parameters most strongly amplifying R_0. An optimal control framework is incorporated into the model with two time dependent control variables: $u_1(t)$, representing preventive and early regulation interventions targeting susceptible and engaged populations, and $u_2(t)$, representing treatment and behavioral support directed at addicted and cognitively dysregulated individuals. The optimal control problem is solved by applying Pontryagin's Maximum Principle. Numerical simulations using the fourth-order Runge-Kutta method demonstrate that the combined application of both controls produces the most significant reduction in social media addiction persistence and its cognitive dysregulation effects over a five-year horizon.

Keywords: Compartmental model, optimal control, social media addiction

1. Introduction

Digital technology has transformed how people connect, share information, and engage with the world, with social media becoming an increasingly central part of daily life [1]. As of 2025, social media users worldwide have exceeded 5.24 billion, with Indonesia alone accounting for approximately 143 million active users, and daily usage averaging 141 minutes, a significant rise from 90 minutes in 2012 [2,3]. Yet this excessive and unregulated use has raised serious concerns about mental health and well-being [4,5]. A particularly pressing consequence is Social Media

*Corresponding author

Addiction (SMA), a pattern of compulsive use marked by loss of behavioral control, withdrawal symptoms, and impaired functioning in social, academic, and occupational life, in ways that parallel behavioral addictions [4]. Research has consistently linked SMA to depression, anxiety, and chronic stress [4,5,6]. Beyond these emotional effects, heavy digital exposure has also been tied to shorter attention spans, weakened working memory, and difficulty with higher order thinking, a cluster of symptoms commonly known as Brain Rot, declared Oxford Word of the Year in 2024 [5,7]. In this study, Brain Rot describes a state of cognitive behavioral dysregulation brought on by excessive digital media consumption, used descriptively rather than as a clinical diagnosis.

Mathematical modeling offers one of the most powerful and systematic approaches for understanding complex phenomena, especially those shaped by interactions among individuals [8]. Among the frameworks most widely adopted in this tradition are compartmental epidemiological models, which have demonstrated remarkable effectiveness in capturing the dynamics of a broad spectrum of infectious diseases, including COVID-19 [9] and tuberculosis [10]. Beyond infectious diseases, such frameworks have been successfully extended to behavioral phenomena, including online game addiction [11] and drug [12]. Building on this tradition, several models have been developed specifically for social media addiction [13,14,15]. Among these, the SEARQ model by Alemneh and Alemu [13] incorporated optimal control strategies for social media addiction, while the SMAD model by Ali et al. [15] examined how social media addiction affects mental health, introducing depression as a compartment that represents a psychological consequence of prolonged addictive engagement. Unlike depression, which is a multifactorial condition arising from a broad range of causes beyond addiction, Brain Rot is conceptualized here as an outcome more narrowly and directly rooted in excessive digital media use itself, manifesting not as affective disturbance but as cognitive impairment affecting attention, working memory, and higher-order functioning, and one that has not yet been formally incorporated into compartmental modeling frameworks. This distinction is further reflected in the model structure, where individuals experiencing cognitive dysregulation continue to influence susceptible individuals rather than being treated as a terminal state, unlike how depression is typically positioned in existing frameworks.

This study therefore builds upon the framework introduced by Ali et al. [15] with two key modifications: the depression compartment is replaced by a Cognitive Dysregulation (Brain Rot) compartment representing progressive cognitive impairment resulting from prolonged addictive exposure, and the transmission mechanism is extended to three active user compartments rather than a single source. For the optimal control component, the approach developed by Alemneh and Alemu [13] serves as a methodological reference. The resulting model comprises six compartments capturing the progression from susceptibility to addiction, cognitive dysregulation, and eventual regulation or disengagement, expressed as a system of nonlinear ordinary differential equations, within which an optimal control framework is embedded to characterize time dependent intervention policies through Pontryagin's Maximum Principle. The study addresses equilibrium analysis, stability, sensitivity

analysis, and numerical simulations of optimal control strategies. The analytical framework follows the methodological structure of Ali et al. [15], adapted to the extended SEABRQ compartmental structure.

2. Theoretical Framework

This section outlines the foundational definitions and theorems that support the analysis of the SEABRQ model, encompassing threshold parameter, equilibrium analysis, local stability, sensitivity analysis, and optimal control theory.

Definition 2.1 ([16]). *Consider the system of differential equations:*

$$\frac{d}{dt}x = f(x), \tag{2.1}$$

where $x \in \mathbb{R}^n$ and $f : E \to \mathbb{R}^n$, with E an open subset of $\mathbb{R}^n$. A point $\bar{x} \in \mathbb{R}^n$ is called an equilibrium point of system (2.1) *if and only if $f(\bar{x}) = 0$.*

Theorem 2.2 ([17]). *Local stability is analyzed using the Jacobian matrix of the linearized system. According to the Routh-Hurwitz criterion, the equilibrium point is locally asymptotically stable if the corresponding Hurwitz conditions are satisfied.*

Definition 2.3 ([18]). *Using the next generation matrix method, the basic reproduction number is given by:*

$$R_0 = \rho(\mathcal{F}\mathcal{V}^{-1}), \tag{2.2}$$

where $\mathcal{F} = \left[\dfrac{\partial \mathcal{F}_i}{\partial x_j}(x_0)\right]$ and $\mathcal{V} = \left[\dfrac{\partial \mathcal{V}_i}{\partial x_j}(x_0)\right]$ denote, respectively, the rate of new infections entering and the net flow rate departing each infected compartment, evaluated at the disease-free equilibrium x_0, and $\rho(\cdot)$ is the spectral radius.

Theorem 2.4 ([16]). *Stability of an equilibrium point can be established using Lyapunov's direct method: if a continuously differentiable function $L(z)$ satisfies $L(z) > 0$ for $z \neq 0$ with $L(0) = 0$, and $\dfrac{dL(z)}{dt} \leq 0$, the equilibrium is Lyapunov stable; if $\dfrac{dL(z)}{dt} < 0$ for all $z \neq 0$, it is asymptotically stable.*

Definition 2.5 ([19]). *The normalized forward sensitivity index of R_0 with respect to a parameter p is expressed as:*

$$\Lambda_p^{R_0} = \frac{\partial R_0}{\partial p} \times \frac{p}{R_0}, \tag{2.3}$$

where p is any parameter incorporated in the model.

Theorem 2.6 ([20]). *For an optimal control problem of the form $\dot{x} = f(x, u, t)$ minimizing $J(u) = \int_{t_0}^{t_f} g(x, u, t)\, dt$, the necessary conditions for optimality are given by Pontryagin's Maximum Principle through a Hamiltonian formulation, comprising the state and costate equations, the optimality condition on the control, and the transversality conditions.*

3. Result and Discussion

3.1. *Model Formulation*

A compartmental model is developed to examine the transmission dynamics of social media addiction along with its cognitive consequence. The total population N(t) is partitioned into six compartments: Susceptible (S): Individuals not yet exhibiting compulsive use but vulnerable to social influence. Engaged (E): Individuals actively using social media in an unstable, non compulsive pattern. Addicted (A): Individuals exhibiting persistent and compulsive social media use characterized by impaired behavioral control. Cognitively Dysregulated (B): Individuals experiencing persistent cognitive behavioral impairment associated with prolonged and excessive digital exposure, conceptually referred to as "brain rot" without implying clinical pathology. Regulated (R): Individuals who have stabilized their social media use into controlled and adaptive patterns, but remain susceptible to relapse. Quit (Q): Individuals who have significantly reduced or disengaged from non essential social media use. The flow between compartments of the SEABRQ model is illustrated in Figure 1.

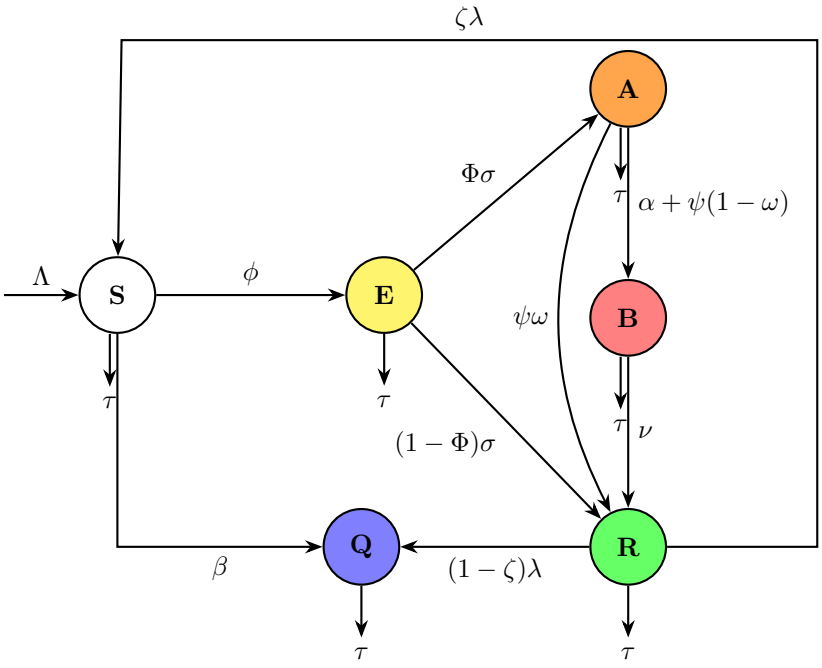

Figure. 1. Compartmental Diagram of SEABRQ model

The dynamics of the system are described by the following set of ordinary differential equations:

$$\begin{cases} \dfrac{dS}{dt} = \Lambda + \zeta\lambda R - \phi\chi(E + A + B)S - (\beta + \tau)S, \\ \dfrac{dE}{dt} = \phi\chi(E + A + B)S - (\sigma + \tau)E, \\ \dfrac{dA}{dt} = \Phi\sigma E - (\tau + \psi + \alpha)A, \\ \dfrac{dB}{dt} = \alpha A + \psi(1 - \omega)A - (\nu + \tau)B, \\ \dfrac{dR}{dt} = (1 - \Phi)\sigma E + \nu B + \psi\omega A - (\tau + \lambda)R, \\ \dfrac{dQ}{dt} = \beta S + (1 - \zeta)\lambda R - \tau Q. \end{cases} \tag{3.1}$$

The initial conditions at time $t = 0$ are assumed to be non-negative:

$$S(0) \geq 0,\ E(0) \geq 0,\ A(0) \geq 0,\ B(0) \geq 0,\ R(0) \geq 0,\ Q(0) \geq 0,$$

with parameter descriptions provided in Table 1. The model employs a density dependent incidence structure, in which the contact rate χ is defined on a per capita basis. This ensures dimensional consistency across all state equations, as the force of infection term $\phi\chi(E + A + B)S$ carries units of people·year^{-1}, matching the units of dS/dt.

3.2. *Invariant Region and Positivity of Solutions*

3.2.1. *Positively invariant region*

To ensure epidemiological feasibility, the dynamics of model (3.1) are studied within the closed set

$$\Delta = \left\{ (S, E, A, B, R, Q) \in \mathbb{R}^6_+ : 0 < N \leq \frac{\Lambda}{\tau} \right\},$$

where $\mathbb{R}^6_+$ denotes the non-negative cone. The set Δ is positively invariant with respect to model (3.1) [13].

Theorem 3.1. *The Δ is positively invariant for model* (3.1).

Proof. Since $N = S + E + A + B + R + Q$, considering the model (3.1) we obtain:

$$\frac{dN}{dt} \leq \Lambda - \tau N.$$

Applying an integrating factor $e^{\tau t}$ to both sides gives:

$$\frac{d}{dt}(e^{\tau t}N) \leq e^{\tau t}\Lambda.$$

Integrating subject to initial conditions yields:

$$N(t) \leq N(0)e^{-\tau t} + \frac{\Lambda}{\tau}(1 - e^{-\tau t}).$$

Taking $t \to \infty$, we obtain $N(t) \leq \frac{\Lambda}{\tau}$. It follows that Δ is positively invariant region for model (3.1). □

Table 1. Values of Parameters

Parameter	**Description**	**Value**	**Source**
Λ	Recruitment rate of susceptible individuals	0.5 people·year^{-1}	[15]
ϕ	Transmission rate of addiction to the susceptible population	0.4	[21]
χ	Contact rate of susceptible individuals with active users (E, A, B)	0.25 people^{-1}·year^{-1}	[13]
β	Rate at which susceptible individuals disengage from active social media use	0.01 year^{-1}	[15]
τ	Natural exit rate	0.1 year^{-1}	[15]
ζ	Proportion of regulated individuals becoming susceptible upon leaving the regulated class	0.35	[22]
λ	Rate at which individuals leave the regulated class	0.4 year^{-1}	[13]
σ	Rate at which individuals leave the exposed class	0.25 year^{-1}	[13]
Φ	Proportion of exposed individuals who become addicted	0.7	[13]
α	Rate at which addicted individuals progress to dysregulated behavior	0.7 year^{-1}	[14]
ψ	Rate at which addicted individuals initiate self-regulation	0.7 year^{-1}	[14]
ω	Probability that self-regulation is successful	0.3	Assume
ν	Rate at which cognitively dysregulated individuals recover through structured intervention	0.8 year^{-1}	Assume

3.2.2. *Positivity of model's solutions*

To ensure epidemiological validity, the non-negativity of all state variables in the model is established [13]. The following theorem guarantees the positivity of the solution to the model.

Theorem 3.2. *Given the initial conditions of model* (3.1)*, the solution is positive for all* $t > 0$.

Proof. From the first equation of system (3.1), it can be shown that:

$$\frac{dS}{dt} \leq \Lambda - (\beta + \tau)S.$$

Applying the integrating factor $e^{(\beta+\tau)t}$ to both sides of equation:

$$e^{(\beta+\tau)t}\frac{dS}{dt} + (\beta + \tau)Se^{(\beta+\tau)t} \leq \Lambda e^{(\beta+\tau)t}.$$

Integrating subject to initial conditions yields:

$$S \leq S(0)e^{-(\beta+\tau)t} + \frac{\Lambda}{\beta+\tau}\left(1 - e^{-(\beta+\tau)t}\right).$$

Taking $t \to \infty$, we obtain $\frac{\Lambda}{\beta+\tau} \geq S(t) \geq 0$. Following the same approach, it can be shown that $E \geq 0,\ A \geq 0,\ B \geq 0,\ R \geq 0,\ Q \geq 0$. Therefore, all state variables of model (3.1) are positive for all $t > 0$. □

3.3. *Equilibrium Points and Threshold Parameter* R_0

The equilibrium points are obtained by setting each equation of system (3.1) equal to zero, yielding two equilibrium points within the feasible region Δ.

3.3.1. *Disease-Free Equilibrium Point (DFE)*

The disease-free equilibrium point is given by:

$$E_{q^0} = (S^0, E^0, A^0, B^0, R^0, Q^0) = \left(\frac{\Lambda}{\beta+\tau},\ 0,\ 0,\ 0,\ 0,\ \frac{\beta\Lambda}{\tau(\beta+\tau)}\right). \tag{3.2}$$

When $R_0 < 1$, the disease-free equilibrium E_{q^0} exists, reflecting a state in which addiction is absent from the population.

3.3.2. *Endemic Equilibrium Point (EEP)*

The endemic equilibrium point is given by:

$$E_{q^1} = (S^1, E^1, A^1, B^1, R^1, Q^1), \tag{3.3}$$

where explicit expressions can be derived as follows:

$$S^1 = \frac{(\sigma+\tau)k_1}{\phi\chi(k_1+1+k_3)},$$

$$E^1 = k_1 \cdot \frac{(\beta+\tau)\cdot\dfrac{(\sigma+\tau)k_1}{\phi\chi(k_1+1+k_3)} - \Lambda}{\zeta\lambda k_2 - (\sigma+\tau)k_1},$$

$$A^1 = \frac{(\beta+\tau)\cdot\dfrac{(\sigma+\tau)k_1}{\phi\chi(k_1+1+k_3)} - \Lambda}{\zeta\lambda k_2 - (\sigma+\tau)k_1},$$

$$B^1 = k_3 \cdot \frac{(\beta+\tau)\cdot\dfrac{(\sigma+\tau)k_1}{\phi\chi(k_1+1+k_3)} - \Lambda}{\zeta\lambda k_2 - (\sigma+\tau)k_1},$$

$$R^1 = k_2 \cdot \frac{(\beta+\tau)\cdot\dfrac{(\sigma+\tau)k_1}{\phi\chi(k_1+1+k_3)} - \Lambda}{\zeta\lambda k_2 - (\sigma+\tau)k_1},$$

$$Q^1 = \frac{1}{\tau}\left[\beta\cdot\frac{(\sigma+\tau)k_1}{\phi\chi(k_1+1+k_3)} + (1-\zeta)\lambda k_2 \cdot \frac{(\beta+\tau)\cdot\dfrac{(\sigma+\tau)k_1}{\phi\chi(k_1+1+k_3)} - \Lambda}{\zeta\lambda k_2 - (\sigma+\tau)k_1}\right],$$

where

$$k_1 = \frac{\tau + \psi + \alpha}{\Phi\sigma},$$
$$k_2 = \frac{\frac{(1-\Phi)(\tau+\psi+\alpha)}{\Phi} + \frac{\nu(\alpha+\psi(1-\omega))}{\nu+\tau} + \psi\omega}{\tau+\lambda},$$
$$k_3 = \frac{\alpha + \psi(1-\omega)}{\nu+\tau}.$$

When $R_0 > 1$, the endemic equilibrium E_{q^1} exists, reflecting the sustained spread of addiction across the population.

3.3.3. *Threshold parameter* R_0

The basic reproduction number R_0 denotes the expected number of new addiction cases generated by one addicted individual during their addictive period in a fully susceptible population. If $R_0 < 1$ addiction dies out, while $R_0 > 1$ indicates endemic persistence. The next generation matrix (NGM) method is employed to derive R_0, through which system (3.1) can be expressed as:

$$\begin{cases} \dfrac{dE}{dt} = \phi\chi(E+A+B)S - \sigma E - \tau E, \\ \dfrac{dA}{dt} = \Phi\sigma E - (\tau+\psi+\alpha)A, \\ \dfrac{dB}{dt} = \alpha A + \psi(1-\omega)A - (\nu+\tau)B, \\ \dfrac{dR}{dt} = (1-\Phi)\sigma E + \nu B + \psi\omega A - (\tau+\lambda)R. \end{cases} \tag{3.4}$$

$$\mathbf{F} = \begin{pmatrix} \phi\chi(E+A+B)S \\ 0 \\ 0 \\ 0 \end{pmatrix}, \quad \mathbf{V} = \begin{pmatrix} (\sigma+\tau)E \\ -\Phi\sigma E + (\tau+\psi+\alpha)A \\ -\alpha A - \psi(1-\omega)A + (\nu+\tau)B \\ -(1-\Phi)\sigma E - \nu B - \psi\omega A + (\tau+\lambda)R \end{pmatrix}.$$

The matrices $\mathcal{F}$ and $\mathcal{V}$ represent the Jacobian of $\mathbf{F}$ and $\mathbf{V}$ evaluated at the disease-free equilibrium, given as follows:

$$\mathcal{F} = \begin{pmatrix} \phi\chi S^0 & \phi\chi S^0 & \phi\chi S^0 & 0 \\ 0 & 0 & 0 & 0 \\ 0 & 0 & 0 & 0 \\ 0 & 0 & 0 & 0 \end{pmatrix}, \quad \mathcal{V} = \begin{pmatrix} \sigma+\tau & 0 & 0 & 0 \\ -\Phi\sigma & \tau+\psi+\alpha & 0 & 0 \\ 0 & -\alpha-\psi(1-\omega) & \nu+\tau & 0 \\ -(1-\Phi)\sigma & -\psi\omega & -\nu & \tau+\lambda \end{pmatrix},$$

where $S^0 = \dfrac{\Lambda}{\beta+\tau}$. The largest eigenvalue of $\mathcal{F}\mathcal{V}^{-1}$ gives the basic reproduction number R_0, expressed as:

$$R_0 = \frac{\Lambda\phi\chi}{(\beta+\tau)(\sigma+\tau)}\left[1 + \frac{\Phi\sigma}{\tau+\psi+\alpha} + \frac{\Phi\sigma[\alpha+\psi(1-\omega)]}{(\tau+\psi+\alpha)(\nu+\tau)}\right]. \tag{3.5}$$

3.4. *Local Stability Analysis*

3.4.1. *Local Stability Analysis of Disease Free Equilibrium Points*

Theorem 3.3. *The disease-free equilibrium point E_{q^0} is locally asymptotically stable if $R_0 < 1$ and unstable if $R_0 > 1$.*

Proof. The Jacobian of System (3.1) evaluated at E_{q^0} in Eq. (3.2) is given by:

$$J(E_{q^0}) = \begin{pmatrix} -(\beta+\tau) & -\frac{\phi\chi\Lambda}{\beta+\tau} & -\frac{\phi\chi\Lambda}{\beta+\tau} & -\frac{\phi\chi\Lambda}{\beta+\tau} & \zeta\lambda & 0 \\ 0 & \frac{\phi\chi\Lambda}{\beta+\tau}-(\sigma+\tau) & \frac{\phi\chi\Lambda}{\beta+\tau} & \frac{\phi\chi\Lambda}{\beta+\tau} & 0 & 0 \\ 0 & \Phi\sigma & -(\tau+\psi+\alpha) & 0 & 0 & 0 \\ 0 & 0 & \alpha+\psi(1-\omega) & -(\nu+\tau) & 0 & 0 \\ 0 & (1-\Phi)\sigma & \psi\omega & \nu & -(\tau+\lambda) & 0 \\ \beta & 0 & 0 & 0 & (1-\zeta)\lambda & -\tau \end{pmatrix}.$$

From $J(E_{q^0})$, four eigenvalues are directly obtained:

$$-\tau,\ -(\nu+\tau),\ -(\tau+\lambda),\ -(\beta+\tau).$$

The remaining eigenvalues are determined from the following quadratic equation:

$$\lambda_1^2 + a_1\lambda_1 + a_2 = 0,$$

$$a_1 = \sigma + 2\tau + \psi + \alpha - \frac{\phi\chi\Lambda}{\beta+\tau}, \quad a_2 = \left(\sigma+\tau-\frac{\phi\chi\Lambda}{\beta+\tau}\right)(\tau+\psi+\alpha) - \frac{\Phi\sigma\phi\chi\Lambda}{\beta+\tau}.$$

By the Routh-Hurwitz criterion, it suffices to show $a_1 > 0$ and $a_2 > 0$.
Let $K = \dfrac{\phi\chi\Lambda}{\beta+\tau}$ and $B = \tau+\psi+\alpha$, so that $R_0 = \dfrac{K}{\sigma+\tau}\cdot H$, where $H = 1 + \dfrac{\Phi\sigma}{B} + \dfrac{\Phi\sigma[\alpha+\psi(1-\omega)]}{B(\nu+\tau)}$.

Showing $a_1 > 0$. Since all parameters are positive and $\omega \in [0,1]$, the term $\alpha+\psi(1-\omega) \geq 0$, so $H \geq 1$, which gives $R_0 \geq \dfrac{K}{\sigma+\tau}$. Therefore $R_0 < 1$ implies $K < \sigma+\tau$, and since $B > 0$: $a_1 = (\sigma+\tau-K) + B > 0$.

Showing $a_2 > 0$. Similarly, since $H \geq 1 + \dfrac{\Phi\sigma}{B}$, we have $R_0 \geq \dfrac{K(B+\Phi\sigma)}{B(\sigma+\tau)}$. Rewriting a_2 explicitly: $a_2 = B(\sigma+\tau) - K(B+\Phi\sigma)$. Then $R_0 < 1$ implies $K(B+\Phi\sigma) < B(\sigma+\tau)$, so $a_2 > 0$.

Since all eigenvalues are negative and Routh-Hurwitz criterion is satisfied, the condition $R_0 < 1$ holds. Therefore, the disease-free equilibrium is locally asymptotically stable. □

3.4.2. *Local Stability Analysis of Endemic Equilibrium Points*

Theorem 3.4. *The endemic equilibrium E_{q^1} is locally asymptotically stable if $R_0 > 1$ and unstable if $R_0 < 1$.*

Proof. By applying Theorem 2.4, the Lyapunov function is constructed:

$$L = \frac{1}{2}(S^2 + E^2 + A^2 + B^2 + R^2 + Q^2).$$

This function is positive definite. Differentiating L with respect to t gives:

$$\frac{dL}{dt} = S\frac{dS}{dt} + E\frac{dE}{dt} + A\frac{dA}{dt} + B\frac{dB}{dt} + R\frac{dR}{dt} + Q\frac{dQ}{dt}.$$

Substituting the derivatives from model (3.1) yields:

$$\begin{aligned}\frac{dL}{dt} &= S(\Lambda + \zeta\lambda R - \phi\chi(E + A + B)S - (\beta + \tau)S) \\ &\quad + E(\phi\chi(E + A + B)S - (\sigma + \tau)E) \\ &\quad + A(\Phi\sigma E - (\tau + \psi + \alpha)A) \\ &\quad + B(\alpha A + \psi(1 - \omega)A - (\nu + \tau)B) \\ &\quad + R((1 - \Phi)\sigma E + \nu B + \psi\omega A - (\tau + \lambda)R) \\ &\quad + Q(\beta S + (1 - \zeta)\lambda R - \tau Q).\end{aligned}$$

Since all parameters and state variables are non-negative, expanding and regrouping into non-positive and non-negative terms, and since the non-positive terms dominate:

$$\begin{aligned}&- \big(\phi\chi(E + A + B)S^2 + (\beta + \tau)S^2 + (\sigma + \tau)E^2 \\ &\quad + (\tau + \psi + \alpha)A^2 + (\nu + \tau)B^2 + (\tau + \lambda)R^2 + \tau Q^2\big) \leq 0\end{aligned}$$

$$\begin{aligned}&\big(S(\Lambda + \zeta\lambda R) + \phi\chi(E + A + B)SE + \Phi\sigma AE + (\alpha A + \psi(1 - \omega))BA \\ &\quad + R((1 - \Phi)\sigma E + \nu B + \psi\omega A) + Q(\beta S + (1 - \zeta)\lambda R)\big) \geq 0.\end{aligned}$$

Therefore, $\dfrac{dL}{dt} \leq 0$ for all non-zero state variables and non-negative parameters of model (3.1), hence the endemic equilibrium E_{q^1} is locally asymptotically stable.□

3.5. *Sensitivity Analysis of the Proposed Model*

Using Definition 2.5 and R_0 given in Eq. (3.5), the sensitivity indices for each parameter are computed below.

$$H = 1 + \frac{\Phi\sigma}{\tau + \psi + \alpha} + \frac{\Phi\sigma[\alpha + \psi(1 - \omega)]}{(\tau + \psi + \alpha)(\nu + \tau)}.$$

(1) Λ, ϕ and χ: $\Lambda_\Lambda^{R_0} = 1 > 0, \quad \Lambda_\phi^{R_0} = 1 > 0, \quad \Lambda_\chi^{R_0} = 1 > 0.$

(2) β: $\Lambda_\beta^{R_0} = -\frac{\beta}{\beta+\tau} < 0.$

(3) σ: $\Lambda_\sigma^{R_0} = \sigma\left[-\dfrac{1}{\sigma + \tau} + \dfrac{\dfrac{\Phi}{\tau + \psi + \alpha} + \dfrac{\Phi[\alpha + \psi(1 - \omega)]}{(\tau + \psi + \alpha)(\nu + \tau)}}{H}\right].$

(4) τ:

$$\Lambda_{\tau}^{R_0} = \tau \left[-\left(\frac{1}{\beta+\tau} + \frac{1}{\sigma+\tau}\right) - \frac{\dfrac{\Phi\sigma}{(\tau+\psi+\alpha)^2} + \Phi\sigma[\alpha+\psi(1-\omega)]\left(\dfrac{1}{(\tau+\psi+\alpha)^2(\nu+\tau)} + \dfrac{1}{(\tau+\psi+\alpha)(\nu+\tau)^2}\right)}{H} \right] < 0.$$

(5) α: $\Lambda_{\alpha}^{R_0} = -\alpha \cdot \dfrac{\dfrac{\Phi\sigma}{(\tau+\psi+\alpha)^2} + \Phi\sigma \cdot \dfrac{(\tau+\psi+\alpha) - [\alpha+\psi(1-\omega)]}{(\tau+\psi+\alpha)^2(\nu+\tau)}}{H}.$

(6) ψ: $\Lambda_{\psi}^{R_0} = -\psi \cdot \dfrac{\dfrac{\Phi\sigma}{(\tau+\psi+\alpha)^2} + \Phi\sigma \cdot \dfrac{(1-\omega)(\tau+\psi+\alpha) - [\alpha+\psi(1-\omega)]}{(\tau+\psi+\alpha)^2(\nu+\tau)}}{H}.$

(7) Φ: $\Lambda_{\Phi}^{R_0} = \Phi \cdot \dfrac{\dfrac{\sigma}{\tau+\psi+\alpha} + \dfrac{\sigma[\alpha+\psi(1-\omega)]}{(\tau+\psi+\alpha)(\nu+\tau)}}{H} > 0.$

(8) ω: $\Lambda_{\omega}^{R_0} = -\omega \cdot \dfrac{\Phi\sigma\psi}{(\tau+\psi+\alpha)(\nu+\tau)H} < 0.$

(9) ν: $\Lambda_{\nu}^{R_0} = -\nu \cdot \dfrac{\Phi\sigma[\alpha+\psi(1-\omega)]}{(\tau+\psi+\alpha)(\nu+\tau)^2 H} < 0.$

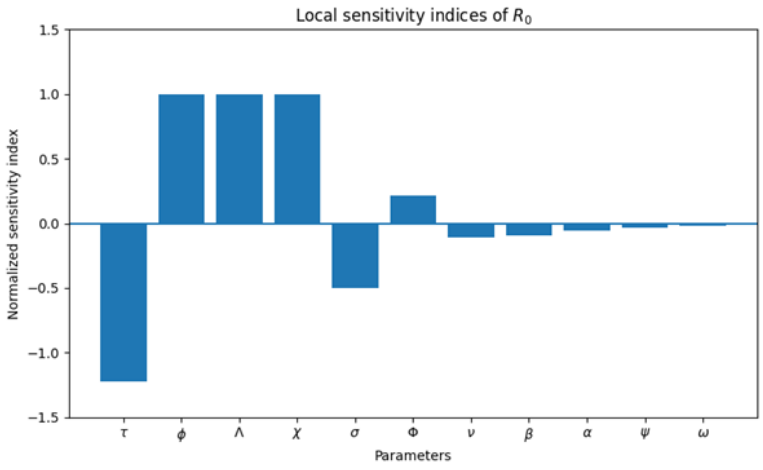

Figure. 2. Local Sensitivity Indices of R_0

The sensitivity indices of R_0 with respect to each model parameter are summarized in Table 2 and visualized in Figure 2. Parameters associated with recruitment and transmission, namely Λ, ϕ, χ, and Φ, yield positive sensitivity indices, indicating that increases in these parameters amplify the basic reproduction number. Conversely, parameters related to removal and recovery processes, including τ, β, ν, ω, α, and ψ, carry negative indices, implying that their increase suppresses R_0.

Table 2. Sensitivity Indices of R_0

Parameter	**Sensitivity Index**	**Value**
τ	$-$	-1.222503
ϕ	$+$	1.000000
Λ	$+$	1.000000
χ	$+$	1.000000
σ	$-$	-0.501114
Φ	$+$	0.213172
ν	$-$	-0.107889
β	$-$	-0.090909
α	$-$	-0.057594
ψ	$-$	-0.036175
ω	$-$	-0.021419

Notably, τ exhibits the strongest negative influence, as it appears in multiple denominator terms of the R_0 formulation an intrinsic feature of the model structure rather than a directly controllable intervention target.

3.6. *Optimal Control Model*

Based on the parameter values given in Table 1, the basic reproduction number is computed as $R_0 \approx 1.6506 > 1$, indicating that social media addiction persists endemically under the current parameter regime. This motivates the incorporation of two time-dependent control variables, $u_1(t)$ and $u_2(t)$. The control $u_1(t)$ represents preventive and digital governance measures targeting susceptible and engaged individuals, reducing effective exposure and redirecting engagement toward regulated usage through interventions such as legislative restrictions on platform access for minors, mandatory ethical design standards, school based smartphone bans, digital literacy programs, and passive behavioral nudges [1,23,24]. The control $u_2(t)$ represents targeted intervention and treatment directed at addicted and cognitively dysregulated individuals, encompassing clinical screening, cognitive behavioral therapy, mindfulness based interventions, and motivational approaches [1,23,24]. The controlled model is expressed as:

$$\begin{aligned}
S' &= \Lambda + \zeta\lambda R - (1-u_1)\phi\chi(E+A+B)S - (\beta+u_1+\tau)S,\\
E' &= (1-u_1)\phi\chi(E+A+B)S - (\sigma+\tau)E,\\
A' &= (1-u_1)\Phi\sigma E - [\tau+\alpha+\psi+u_2]A,\\
B' &= \alpha A + \psi(1-\omega)A - (\nu+u_2+\tau)B,\\
R' &= (1-\Phi)\sigma E + u_1\Phi\sigma E + \psi\omega A + u_2 A + (\nu+u_2)B - (\tau+\lambda)R,\\
Q' &= (\beta+u_1)S + (1-\zeta)\lambda R - \tau Q,
\end{aligned} \tag{3.6}$$

$$0 \le u_i(t) \le 1, \quad i = 1, 2.$$

The objective function is defined as follows:

$$J(u_1, u_2) = \int_0^{t_f} \left[q_1 A(t) + q_2 B(t) + \frac{1}{2}(r_1 u_1^2 + r_2 u_2^2) \right] dt, \tag{3.7}$$

where t_0 and t_f are the initial and final times, q_i are positive weight for the state variables, and r_i are positive costs coefficients for the control functions.

Based on Pontryagin's Maximum Principle Theorem 2.6, the Hamiltonian function is constructed as follows:

$$\begin{aligned}
\mathcal{H} = {} & q_1 A + q_2 B + \frac{1}{2}(r_1 u_1^2 + r_2 u_2^2) \\
& + \lambda_1[\Lambda + \zeta\lambda R - (1-u_1)\phi\chi(E+A+B)S - (\beta + u_1 + \tau)S] \\
& + \lambda_2[(1-u_1)\phi\chi(E+A+B)S - (\sigma+\tau)E] \\
& + \lambda_3[(1-u_1)\Phi\sigma E - [\tau + \alpha + \psi + u_2]A] \\
& + \lambda_4[\alpha A + \psi(1-\omega)A - (\nu + u_2 + \tau)B] \\
& + \lambda_5[(1-\Phi)\sigma E + u_1\Phi\sigma E + \psi\omega A + u_2 A + (\nu + u_2)B - (\tau + \lambda)R] \\
& + \lambda_6[(\beta + u_1)S + (1-\zeta)\lambda R - \tau Q].
\end{aligned}$$

From the Hamiltonian, the state and costate systems are derived, with the state equations given by:

$$\begin{aligned}
\frac{\partial H}{\partial \lambda_1} &= \Lambda + \zeta\lambda R - (1-u_1)\phi\chi(E+A+B)S - (\beta + u_1 + \tau)S, \\
\frac{\partial H}{\partial \lambda_2} &= (1-u_1)\phi\chi(E+A+B)S - (\sigma+\tau)E, \\
\frac{\partial H}{\partial \lambda_3} &= (1-u_1)\Phi\sigma E - [\tau + \alpha + \psi + u_2]A, \\
\frac{\partial H}{\partial \lambda_4} &= \alpha A + \psi(1-\omega)A - (\nu + u_2 + \tau)B, \\
\frac{\partial H}{\partial \lambda_5} &= (1-\Phi)\sigma E + u_1\Phi\sigma E + \psi\omega A + u_2 A + (\nu + u_2)B - (\tau + \lambda)R, \\
\frac{\partial H}{\partial \lambda_6} &= (\beta + u_1)S + (1-\zeta)\lambda R - \tau Q,
\end{aligned}$$

With initial condition:

$$S(0) = S_0,\ E(0) = E_0,\ A(0) = A_0,\ B(0) = B_0,\ R(0) = R_0,\ Q(0) = Q_0.$$

From the Hamiltonian, the costate equations are given by:

$$\begin{aligned}
\frac{d\lambda_1}{dt} &= (1-u_1)\phi\chi(E+A+B)(\lambda_1 - \lambda_2) + (\beta + u_1 + \tau)\lambda_1 - (\beta + u_1)\lambda_6, \\
\frac{d\lambda_2}{dt} &= (1-u_1)\phi\chi S(\lambda_1 - \lambda_2) + (\sigma+\tau)\lambda_2 - (1-u_1)\Phi\sigma\lambda_3 - \sigma[(1-\Phi) + u_1\Phi]\lambda_5, \\
, \frac{d\lambda_3}{dt} &= -q_1 + (1-u_1)\phi\chi S(\lambda_1 - \lambda_2) + (\tau + \alpha + \psi + u_2)\lambda_3 - [\alpha + \psi(1-\omega)]\lambda_4 - (\psi\omega + u_2)\lambda_5,
\end{aligned}$$

$$\frac{d\lambda_4}{dt} = -q_2 + (1-u_1)\phi\chi S(\lambda_1 - \lambda_2) + (\nu + u_2 + \tau)\lambda_4 - (\nu + u_2)\lambda_5,$$
$$\frac{d\lambda_5}{dt} = -\zeta\lambda\lambda_1 + (\tau + \lambda)\lambda_5 - (1-\zeta)\lambda\lambda_6,$$
$$\frac{d\lambda_6}{dt} = \tau\lambda_6.$$

The optimal controls $u_1^*(t)$ and $u_2^*(t)$ are given by:

$$u_1^*(t) = \max\left\{0, \min\left(1, \frac{\phi\chi(E+A+B)S(\lambda_2-\lambda_1) + \Phi\sigma E(\lambda_3-\lambda_5) + S(\lambda_1-\lambda_6)}{r_1}\right)\right\},$$
$$u_2^*(t) = \max\left\{0, \min\left(1, \frac{A(\lambda_3-\lambda_5) + B(\lambda_4-\lambda_5)}{r_2}\right)\right\}.$$

3.7. *Numerical Simulation*

The fourth-order Runge-Kutta method is employed to run numerical simulations, aimed at assessing the effectiveness of the proposed control strategies in reducing social media addiction and cognitive dysregulation, implemented in Google Colab. The parameter values are as listed in Table 1 with initial conditions $S(0) = 1000$, $E(0) = 10$, $A(0) = 50$, $B(0) = 50$, $R(0) = 0$, $Q(0) = 10$, over a time interval of $t_0 = 0$ to $t_f = 5$ years. The weighting constants for the addicted and cognitively dysregulated compartments are set to $q_1 = q_2 = 1$, and the control cost weights are $r_1 = r_2 = 10$.

Three control strategies are considered in numerical simulation:

Strategy A: Preventive and Early-Regulation Control ($u_1 \neq 0$, $u_2 = 0$)

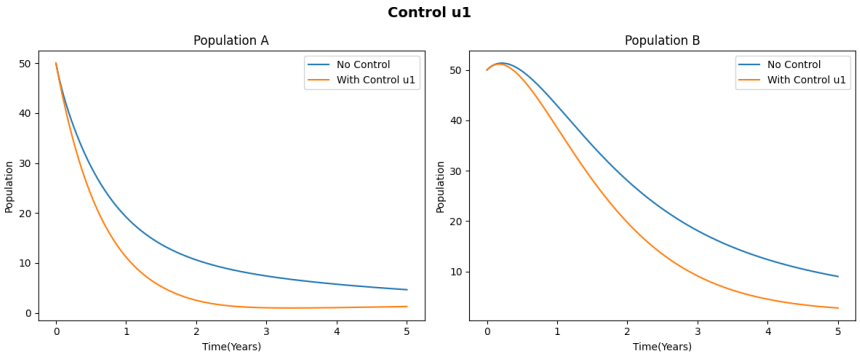

Figure. 3. Population dynamics of A and B under Strategy A (control u_1)

Figure 3 shows the dynamics of the addicted (A) and cognitively dysregulated (B) compartments under Strategy A, where only u_1 is activated. Both compartments decline faster than the no-control scenario. Since u_1 works upstream by reducing exposure and redirecting individuals before addiction develops, its strongest effect

is in slowing new entries into A, which in turn limits progression into B. Because u_1 does not directly target those already in A or B, recovery among already affected individuals remains gradual, making this strategy more suitable for prevention than for treatment.

Strategy B: Intervention and Treatment Control ($u_1 = 0$, $u_2 \neq 0$)

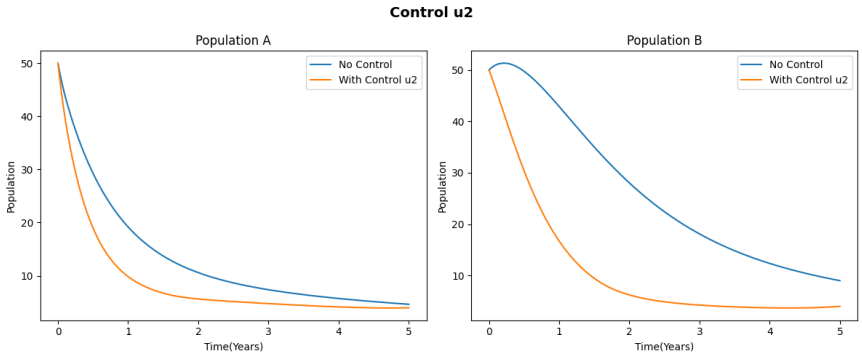

Figure. 4. Population dynamics of A and B under Strategy B (control u_2)

Figure 4 shows the dynamics under Strategy B, where only u_2 is active. Since u_2 directly increase transition rates from A and B toward the regulated compartment R, a marked acceleration in recovery is observed in both populations, with suppression of Strategy B appearing more immediate than under Strategy A. However, as Strategy B does not address upstream transmission, new entries into A continue uninterrupted, potentially limiting its long term effectiveness without concurrent preventive measures.

Strategy C: Combined Control ($u_1 \neq 0$, $u_2 \neq 0$)

Figure 5 shows the dynamics under Strategy C, where both controls are applied simultaneously. This combined strategy produces the greatest and most sustained reduction in both A and B, as u_1 reduces new infections while u_2 speeds up recovery toward regulated behavior. These results confirm that combining both interventions is more effective than applying either one alone, highlighting the need to pair preventive digital governance policies with accessible treatment programs for those already affected.

4. Conclusion

This study constructs a SEABRQ compartmental model to analyze social media addiction and its cognitive consequence, featuring a Cognitively Dysregulated compartment(B) and three active transmission sources (E, A, B). The basic reproduction number $R_0 > 1$, obtained through the next generation matrix, suggests

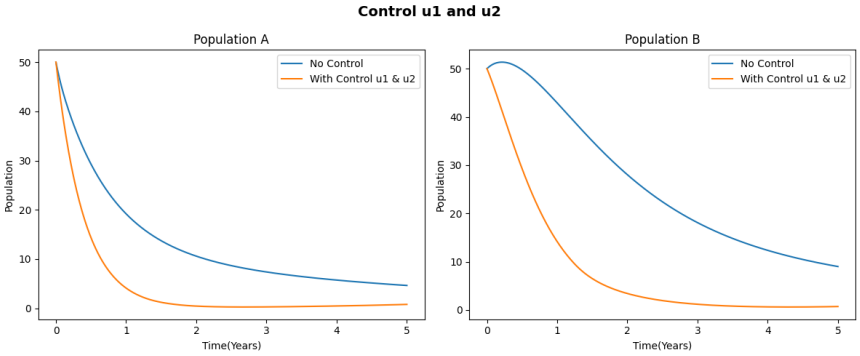

Figure. 5. Population dynamics of A and B under Strategy C (control u_1 and u_2)

endemic potential under the chosen parameter values, indicates that addiction can persist in a population without intervention. This is consistent with how peer influence and algorithmic exposure sustain compulsive use. Local asymptotic stability of the addiction-free equilibrium holds when $R_0 < 1$, while the endemic equilibrium is stable when $R_0 > 1$, verified through Routh-Hurwitz conditions and Lyapunov's theorem. Sensitivity analysis revealed that Λ, ϕ, χ, and Φ increase R_0, while τ, β, ν, ω, α, and ψ reduce it. These results motivated two optimal controls: $u_1(t)$for prevention through digital governance, and $u_2(t)$ for treatment and recovery. Numerical simulations over a five year horizon confirm that Strategy C, combining both controls, yields the greatest and most sustained reduction in compartments A and B, confirming that integrating both preventive and treatment approaches achieves more substantial reductions than either control applied independently.

Future work may incorporate psychological predispositions or multi platform addiction scenarios to better capture individual variability in addiction susceptibility. Calibrating the model with real-world demographic data would enhance its practical relevance for public health policy.

5. Acknowledgment

The authors would like to express their sincere gratitude to Universitas Ahmad Dahlan for the institutional support provided throughout the course of this research.

Bibliography

[1] D. Deckker and S. Sumanasekara. A systematic review of the impact of artificial intelligence, digital technology, and social media on cognitive functions. *International Journal of Research and Innovation in Social Science*, IX(III):134–154, 2025.

[2] S. Kemp. Digital 2025: Global Overview Report. `https://datareportal.com/reports/digital-2025-global-overview-report`, 2025. [Accessed 14-04-2026].

[3] D. Thuy. Average daily time spent on social media worldwide 2012-2025. `https://www.statista.com/statistics/433871/`

daily-social-media-usage-worldwide/, November 2025. [Accessed 14-04-2026].

[4] S.Y. Tereshchenko. Neurobiological risk factors for problematic social media use as a specific form of internet addiction: A narrative review. *World Journal of Psychiatry*, 13(5):160–173, May 2023.

[5] E. Harsanto, Y. Yunike, and I. Kusumawaty. Brain rot and focus disorders survey impact of consumption of tiktok and instagram reels content on teenagers. *International Journal Scientific and Professional*, 4(3):593–600, 2025.

[6] J. Fox and J.J. Moreland. The dark side of social networking sites: An exploration of the relational and psychological stressors associated with facebook use and affordances. *Computers in Human Behavior*, 45:168–176, April 2015.

[7] A.M.F. Yousef, A. Alshamy, A. Tlili, and A.H.S. Metwally. Demystifying the new dilemma of brain rot in the digital era: A review. *Brain Sciences*, 15(3):283, March 2025.

[8] A. Baca, D. Gonzalez, A.G.. Ogueda, H.C. Matto, and P. Seshaiyer. Mathematical modeling, analysis, and simulation of patient addiction journey. *CODEE Journal*, 18(1):1–20, 2024.

[9] K. Khoerunnisa and Y.A. Adi. Masalah kontrol optimal pada penyebaran covid-19 di jawa tengah dengan vaksinasi. *Jurnal Matematika UNAND*, 10(4):538–552, October 2021.

[10] Z. Nafisah and Y.A. Adi. Model seir dengan pseudo-recovery pada kasus tuberkulosis di jawa barat. *Jurnal Matematika UNAND*, 13(3):170–187, July 2024.

[11] A. Saman, S. Side, M.I. Pratama, and W. Sanusi. Optimal control of the seir model of online game addiction using guidance and counseling. *Engineering Letters*, 30(3):27–31, 2022.

[12] A. Zakiyyah and S. Bahri. Stability analysis of drug abuse transmission dynamics. *Jurnal Matematika UNAND*, 14(1):103–116, January 2025.

[13] H.T. Alemneh and N.Y. Alemu. Mathematical modeling with optimal control analysis of social media addiction. *Infectious Disease Modelling*, 6:405–419, 2021.

[14] J. Juhari, E. Alisah, A.A. Safitri, and I. Sujarwo. Optimal control of a modified mathematical model of social media addiction. *InPrime: Indonesian Journal of Pure and Applied Mathematics*, 6(2):112–123, October 2024.

[15] A.S. Ali, S. Javeed, Z. Faiz, and D. Baleanu. Mathematical modelling, analysis and numerical simulation of social media addiction and depression. *PLOS ONE*, 19(3):e0293807, March 2024.

[16] L. Perko. *Differential Equations and Dynamical Systems*. Texts in Applied Mathematics. Springer New York, 2001.

[17] J.D. Murray. *Mathematical Biology: I. An Introduction*. Interdisciplinary Applied Mathematics. Springer, New York, 3 edition, 2002.

[18] P. van den Driessche and J. Watmough. Reproduction numbers and subthreshold endemic equilibria for compartmental models of disease transmission. *Mathematical Biosciences*, 180(1–2):29–48, November 2002.

[19] N. Chitnis, J. M. Hyman, and J. M. Cushing. Determining important parameters in the spread of malaria through the sensitivity analysis of a mathematical model. *Bulletin of mathematical biology*, 70(5):1272–1296, 2008.

[20] L.S. Pontryagin. *Mathematical Theory of Optimal Processes*. Classics of Soviet

Mathematics. Taylor & Francis, 1987.

[21] Y. Guo and T. Li. Optimal control and stability analysis of an online game addiction model with two stages. *Mathematical Methods in the Applied Sciences*, January 2020.

[22] J. Kongson, W. Sudsutad, C. Thaiprayoon, J. Alzabut, and C. Tearnbucha. On analysis of a nonlinear fractional system for social media addiction involving atangana–baleanu–caputo derivative. *Advances in Difference Equations*, 2021(1), July 2021.

[23] H. Shannon, M. Montgomery, A. Funk, A. Kamyabi, M. Hunt, C. Pope, K. Hellemans, and S. Guimond. Beyond problematic social media use and the brain: A public health and policy perspective. *Annals of the New York Academy of Sciences*, 1550(1):14–22, June 2025.

[24] R. Hidayat and M. N. Wangid. Phenomenology: Brain rot in gen z reviewed from the perspective of the cognitive behavioral therapy (cbt) approach. *World Psychology*, 4(1):135–148, 2025.